

# Telegraph signals as a solution of the time dependent Schrödinger equation

D. Drakova

*University of Sofia, Faculty of Chemistry, Sofia, Bulgaria\**

G. Doyen

*Ludwig-Maximilians University, Munich, Germany†*

## Abstract

A particle switching between two sides of a symmetric system in interaction with a continuum exhibits a telegraph-like time development without the need of the Born-Bohr principle of reduction on eigenstates of the measuring equipment. The origin of the telegraph signal is a very weak local coupling of the particle to the continuum which is connected with an enormous slow down of the particle motion. The proposed mechanism might serve as a useful simple model for studying decoherence effects due to coupling to the environment.

PACS numbers: 03.70.+k, 11.10.-z, 03.65.Ud, 42.50.Lc, 73.20.Fz, 03.65.Yz

---

\*Electronic address: drakova@inorg.chem.uni-sofia.bg

†URL: <http://www.cenat.de/>

## I. INTRODUCTION

Telegraph signals have been observed in experiments of very different nature. They are displayed as sudden changes of a measured signal between two or more values with time, appearing in a random, statistical manner (cf. for instance [1]-[9]).

The common theoretical approaches to random telegraph signals involve stochastic elements and range from hidden Markov models, to Marcus theory and classical or quantum stochastic approaches [10] (more details are found in ref. [11]). The Bohr-Born concept of state reduction [12] is implied by the state-of-the-art decoherence theory where permanent "measurement" by the environment of a local system is assumed to lead to special pointer states, into which the system collapses. Within collapse theories the explanation of the statistical change of the state of a measured local system relies on truncation of the coherent time development, as it is described with the time dependent Schrödinger equation. Between two collapses the local system evolves coherently, at random time intervals it collapses on one or another eigenstate of the "measuring" environment. There is no approach, to our knowledge, based on a pure coherent time development as Schrödinger's equation requires, leading to a coherent telegraph-signal-like behaviour of a quantum system.

The question is: can a coherent quantum mechanical description of a local system in interaction with the environment lead to the telegraph signal. In the present paper we give a positive answer to this question. We demonstrate that it is possible for a system, comprising a local part, entangled to the continua of the environmental excitations, to change state suddenly in an apparently statistical fashion, which comes out of the solution of the time dependent Schrödinger equation. The conditions for a telegraph-signal-like change of state of the system are weak and local coupling to a continuum of environmental excitations exhibiting soft modes. The time development is coherent and deterministic in the phase space of the total system including the environmental excitations. Focusing on the time development of the local system alone, which is assumed to be accessible to measurement in experiment, it appears as if it changes state in a random way.

In the next section we define the model and the Hamiltonian. Next the method of solution

is outlined, followed by presenting the results and their discussion.

## II. HAMILTONIAN

The model describes an object called "particle" which moves in a universe consisting of two sides, side  $\alpha$  and side  $\beta$ . We want to investigate how long does it take for the "particle" to get from one side to the other, i.e. the dynamics of side change. In the present article we specify neither the "particle" nor the physical nature of the environmental excitations. "Particles" like an electron or an adsorbed atom and the environmental continua of electron-hole pairs, phonons, etc. may be envisioned.

On each side of the universe we have the same number and kind of states in which the "particle" can reside:

1. One remote state  $|g_\alpha\rangle$  and  $|g_\beta\rangle$ , respectively. From these remote states the "particle" can get to the gateway states  $|w_\alpha\rangle$  on the same side or  $|w_\beta\rangle$  on the other side.
2. One gateway state  $|w_\alpha\rangle$  or  $|w_\beta\rangle$ . From these gateway states the "particle" can either get to the environmental states  $\{| \kappa_\alpha \rangle\}$  or  $\{| \kappa_\beta \rangle\}$  on the same side or to the remote state  $|g_\alpha\rangle$  on the same side or on the opposite side  $|g_\beta\rangle$ .
3.  $N$  environmental states  $\{| \kappa_\alpha \rangle\}$  or  $\{| \kappa_\beta \rangle\}$ . The number  $N$  is large compared to unity and limited only by the computational power. From the environmental states the "particle" can only get back to the gateway state on the same side.

The explicit form of the Hamiltonian is:

$$\begin{aligned}
H &= H_\alpha + H_\beta + H_{\alpha-\beta} \\
H_\alpha &= E_g n_{g\alpha} + E_w n_{w\alpha} + \sum_{\kappa} \varepsilon_{\kappa} n_{\kappa\alpha} + V(c_{g\alpha}^+ c_{w\alpha} + h.c.) \\
&\quad + W \sum_{\kappa} (c_{\kappa\alpha}^+ c_{w\alpha} + h.c.) \\
H_\beta &= E_g n_{g\beta} + E_w n_{w\beta} + \sum_{\kappa} \varepsilon_{\kappa} n_{\kappa\beta} + V(c_{g\beta}^+ c_{w\beta} + h.c.) \\
&\quad + W \sum_{\kappa} (c_{\kappa\beta}^+ c_{w\beta} + h.c.) \\
H_{\alpha-\beta} &= (V - \Delta V)(c_{g\alpha}^+ c_{w\beta} + c_{g\beta}^+ c_{w\alpha} + h.c.)
\end{aligned} \tag{1}$$

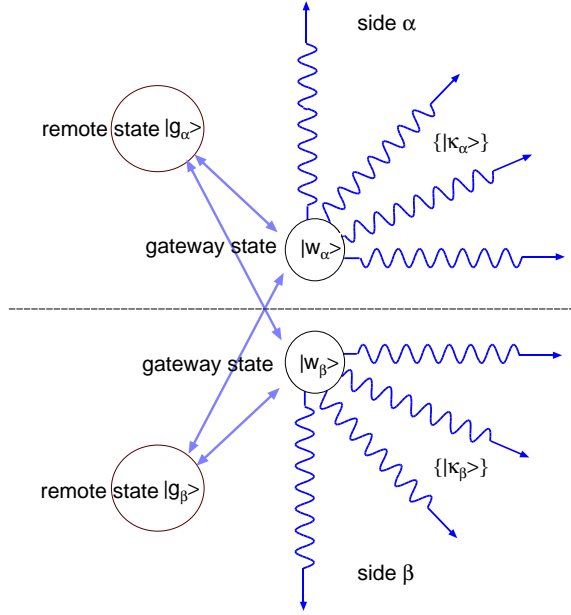


FIG. 1: Model of two remote states of a "particle"  $|g_\alpha\rangle, |g_\beta\rangle$ , coupling within two gateway states  $|w_\alpha\rangle, |w_\beta\rangle$  to the environmental states  $\{| \kappa_\alpha\rangle\}, \{| \kappa_\beta\rangle\}$ .

where  $E_g$  and  $E_w$  are the single-particle energies of the degenerate remote states  $|g_\alpha\rangle, |g_\beta\rangle$  and the gateway states  $|w_\alpha\rangle, |w_\beta\rangle$ , respectively.  $\varepsilon_\kappa$  are the energies of the environmental states.  $n_{g\alpha}$  and  $n_{w\alpha}$  are occupation number operators for the "particle" in the states  $|g_\alpha\rangle, |w_\alpha\rangle$ ;  $c_{g\alpha}^+, c_{g\alpha}, c_{w\alpha}^+, c_{w\alpha}$ : creation and destruction operators for the "particle" in the respective states;  $c_{\kappa\alpha}^+$  and  $c_{\kappa\alpha}$ : creation and destruction operators for the "particle" in the environmental states coupling to the gateway states;  $V$  and  $V - \Delta V$ : interaction matrix element between the remote states and the gateway states;  $W$ : interaction matrix elements between a gateway state and the environmental states it couples to. The states  $\{| \kappa_\alpha\rangle\}, \{| \kappa_\beta\rangle\}$  constitute a quasi-continuum which is modified due to entanglement to the states  $|w_\alpha\rangle, |w_\beta\rangle$ . The coupling of the "particle" to the environmental states is weak and it is mediated by the gateway states.

### A. Solution method: coherent time evolution of a "particle" entangled with a continuum of environmental states

The time evolution of the "particle" is according to Schrödinger's time-dependent equation:

$$i\hbar \frac{d\Psi(t)}{dt} = H\Psi(t) \quad (2)$$

with  $\Psi$  an eigenfunction of the total Hamiltonian eq. (1). The eigenfunctions  $\Psi_I$ , determined by an expansion in the basis states, are used to derive the time dependence according to the unitary time evolution:

$$\Psi_I(t) = \Psi_I(t_0)e^{-iE_I t/\hbar} \quad (3)$$

Assume that the "particle" starts in  $|g_\alpha\rangle$ . The "particle" state, expanded in the eigenfunctions  $\{|I\rangle\}$  of the total Hamiltonian at time  $t_0 = 0$  is:

$$|g_\alpha(t_0)\rangle = c_{1,g_\alpha} |1\rangle + c_{2,g_\alpha} |2\rangle + \dots \quad (4)$$

where  $c_{I,g_\alpha}$  is the linear coefficient of the remote state  $|g_\alpha\rangle$  in the  $I$ -th eigenfunction of the Hamiltonian. The time development of  $|g_\alpha\rangle$  is obtained as:

$$|g_\alpha(t_1)\rangle = c_{1,g_\alpha} e^{-iE_1 t_1/\hbar} |1\rangle + c_{2,g_\alpha} e^{-iE_2 t_1/\hbar} |2\rangle + \dots \quad (5)$$

The density operator, represented in the input basis, at time  $t_1$  is:

$$\rho(t_1) = |g_\alpha(t_1)\rangle\langle g_\alpha(t_1)| \quad (6)$$

Repeating this procedure for each next time step provides the coherent time evolution of the density operator (in the input basis) which can be used to illustrate the state changes of the "particle" in interaction with the continuum of environmental states.

## III. RESULTS

We provide three numerical examples with 800 continuum states. The parameters are summarized in table I. Results of these calculations are plotted in fig. 2.

TABLE I: Parameter values used for the results displayed in fig. 2.

example	$E_g$ [peV]	$E_w$ [peV]	$\Delta\varepsilon$ [peV]	$V$ [peV]	$W$ [peV]	$\Delta V$ [peV]
1 example	0.00	2.50	$2.22 \times 10^{-6}$	0.05	0.00707	0.045
2 example	0.00	2.50	$2.22 \times 10^{-6}$	0.05	0.00707	0.018
3 example	0.00	2.50	$2.22 \times 10^{-6}$	0.05	0.00707	0.005

The time development of the system without entanglement to the environmental states (i.e.  $W = 0$ ) is displayed in the left panels of fig. 2 for the three examples. The quantity plotted is the occupation of side  $g_\alpha$ :

$$\langle g_\alpha | \rho(t) | g_\alpha \rangle + \langle w_\alpha | \rho(t) | w_\alpha \rangle \quad (7)$$

as a function of time.

The system starts on the  $\alpha$ -side with the "particle" occupying the state  $|g_\alpha\rangle$ . The time development of the system is the result of solving Schrödinger's time dependent equation as it is described in the previous section II A and in refs. [13, 14]. Within a certain time interval, which depends on the coupling strength between the states  $|g_\alpha\rangle$ ,  $|g_\beta\rangle$  and  $|w_\alpha\rangle$ ,  $|w_\beta\rangle$ , the occupation of side  $\alpha$  reduces and the particle changes side to  $\beta$ . The stronger the coupling between the remote states and the gateway states is, the faster the particle changes from one side to the other. It is obvious though, that the changes of the side occupation with time are sine-like, rather than telegraph-signal-like. These are just coherent Rabi oscillations between the two sides  $|g_\alpha\rangle$  and  $|g_\beta\rangle$ , mediated by coupling to the gateway states  $|w_\alpha\rangle$  and  $|w_\beta\rangle$ . The frequency of side transition is determined by the energy difference  $\Delta\varepsilon$  between the eigenstates of the system involving the remote states and the gateway states only:  $|g_\alpha\rangle$ ,  $|g_\beta\rangle$ ,  $|w_\alpha\rangle$ ,  $|w_\beta\rangle$ .

Only with entanglement to the environmental states included, does a telegraph-signal-like time development of the side switching arise as it is seen on the central panel of fig. 2, where the changes of the occupation of side  $g_\alpha$  are plotted as a function of time:

$$\langle g_\alpha | \rho(t) | g_\alpha \rangle + \langle w_\alpha | \rho(t) | w_\alpha \rangle + \sum_{\kappa\alpha} \langle \kappa_\alpha | \rho(t) | \kappa_\alpha \rangle \quad (8)$$

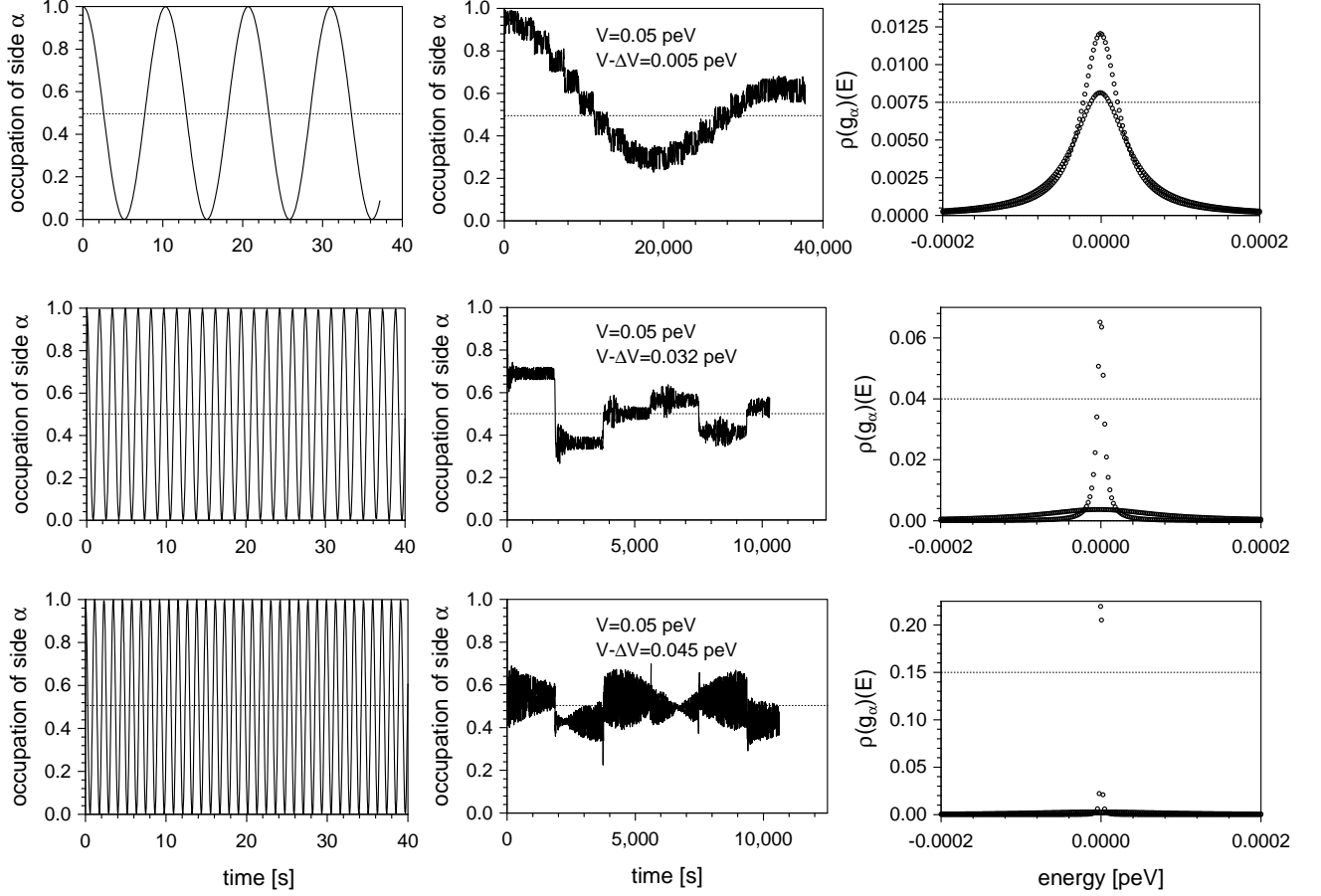


FIG. 2: Left panels: Coherent Rabi oscillations of the "particle" between the two sides  $\alpha$  and  $\beta$  in fig. 1 determine the side variation with time. No entanglement to environmental states within the gateway states is included. The occupation of side  $\alpha$  (eq. 7) is plotted as a function of time. Central panels: Switching of the "particle" between the sides  $\alpha$  and  $\beta$  results with the entanglement to the environmental states  $\{|\kappa_\alpha\rangle\}$  and  $\{|\kappa_\beta\rangle\}$  within the gateway states  $|w_\alpha\rangle, |w_\beta\rangle$  taken into account. The time development of the occupation of side  $\alpha$  eq. (8) is plotted. Right panels: Spectral distribution of  $|g_\alpha\rangle$  within the band of environmental states (eq. 16). The telegraph signal in the middle central panel is provided by the time development of the component  $|g-\rangle$  (fig. 3).

The telegraph-like change of side is observed only in the second row, central panel with the choice of the coupling parameter between the remote states and the gateway states  $V - \Delta V = 0.032$  peV.

The eigenstates  $\{| I \rangle\}$  are obtained by diagonalizing numerically a  $800 \times 800$ -matrix representing the Hamiltonian. An apparently statistical telegraph-like change of side of the "particle" is observed in the second example, displayed in the middle central panel in fig. 2. Furthermore, a significant slow down of the switching rate between the sides results, compared to the period of the Rabi oscillation, neglecting the entanglement to environmental states (cf. fig. 2, left and central panels). In the telegraph regime the average frequency of the telegraph signal is determined by a much smaller energy difference  $\Delta\varepsilon = 2.2 \times 10^{-6}$  peV equal to the energy separation of the environmental states which entangle to the "particle" movement.

## IV. DISCUSSION

### A. Symmetry adapted basis states

The model system is obviously symmetric with respect to interchanging the indices  $\alpha$  and  $\beta$ , i.e., interchanging the two sides. The eigenstates are therefore either symmetric or anti-symmetric with respect to such an interchange. We therefore make the following transformation:

$$\begin{aligned} c_{g+} &= \frac{1}{\sqrt{2}}(c_{g\alpha} + c_{g\beta}) \\ c_{g-} &= \frac{1}{\sqrt{2}}(c_{g\alpha} - c_{g\beta}) \\ c_{w+} &= \frac{1}{\sqrt{2}}(c_{w\alpha} + c_{w\beta}) \\ c_{w-} &= \frac{1}{\sqrt{2}}(c_{w\alpha} - c_{w\beta}) \end{aligned} \tag{9}$$

The coupling matrix elements are then:

$$\begin{aligned} \langle g_+ | H | w_+ \rangle &= \frac{1}{2}(4V - 2\Delta V) = 2V - \Delta V \\ \langle g_+ | H | w_- \rangle &= \frac{1}{2}(V - V - V + \Delta V + V - \Delta V) = 0 \\ \langle g_- | H | w_+ \rangle &= 0 \\ \langle g_- | H | w_- \rangle &= \frac{1}{2}(V + V - V + \Delta V - V + \Delta V) = \Delta V \end{aligned} \tag{10}$$

Transformed operators for environmental states are defined as:

$$c_{\kappa+} = \frac{1}{\sqrt{2}}(c_{\kappa\alpha} + c_{\kappa\beta})$$



$$c_{\kappa-} = \frac{1}{\sqrt{2}}(c_{\kappa\alpha} - c_{\kappa\beta}) \quad (11)$$

The coupling matrix elements between the gateway states and the environmental states are then:

$$\begin{aligned} \langle w_+ | H | \kappa_+ \rangle &= \frac{1}{2}(W + W) = W \\ \langle w_- | H | \kappa_+ \rangle &= 0 \\ \langle w_+ | H | \kappa_- \rangle &= 0 \\ \langle w_- | H | \kappa_- \rangle &= \frac{1}{2}(W + W) = W \end{aligned} \quad (12)$$

With these transformed operators the Hamiltonian reads:

$$\begin{aligned} H &= H_+ + H_- \\ H_+ &= E_g n_{g+} + E_w n_{w+} + \sum_{\kappa} \varepsilon_{\kappa} n_{\kappa+} \\ &\quad + (2V - \Delta V)(c_{g+}^+ c_{w+} + c_{w+}^+ c_{g+}) + W \sum_{\kappa} (c_{\kappa+}^+ c_{w+} + c_{w+}^+ c_{\kappa+}) \\ H_- &= E_g n_{g-} + E_w n_{w-} + \sum_{\kappa} \varepsilon_{\kappa} n_{\kappa-} \\ &\quad + \Delta V(c_{g-}^+ c_{w-} + c_{w-}^+ c_{g-}) + W \sum_{\kappa} (c_{\kappa-}^+ c_{w-} + c_{w-}^+ c_{\kappa-}) \end{aligned} \quad (13)$$

The consequence is that the  $\{|\kappa+\rangle\}$  and  $\{|\kappa-\rangle\}$  systems are decoupled. The mixing between the remote state and the on-shell environmental states is weaker in the antisymmetric system, if  $\Delta V$  is significantly smaller than  $(2V - \Delta V)$ , i.e. in the telegraph and bonding regimes (see below). The interactions in each system are illustrated in fig. 3 for this situation. The degeneracy between the continua  $\{|\kappa+\rangle\}$  and  $\{|\kappa-\rangle\}$  is lifted because of the different remote state - gateway state coupling in the  $\{+\}$  and  $\{-\}$  subsystems. If  $\Delta V$  is small and the time development of the "particle" starts from  $|g_{\alpha}\rangle$  then the "particle" in the  $|g-\rangle$ -component alone stays approximately on-shell and, due to the weakness of the interaction  $W$ , mixes significantly with the on-shell environmental states. The energy shell is defined by the energy of the "particle" in its initial state  $|g_{\alpha}\rangle$ . This energy is set equal to zero. This means that  $|g_{\alpha}\rangle$  mixes in only with the  $\{|\kappa-\rangle\}$  continuum because  $\{|\kappa+\rangle\}$  and  $\{|\kappa-\rangle\}$  states are not mixed and only states belonging to  $\{|\kappa-\rangle\}$  are nearly on-shell with  $|g_{\alpha}\rangle$ .

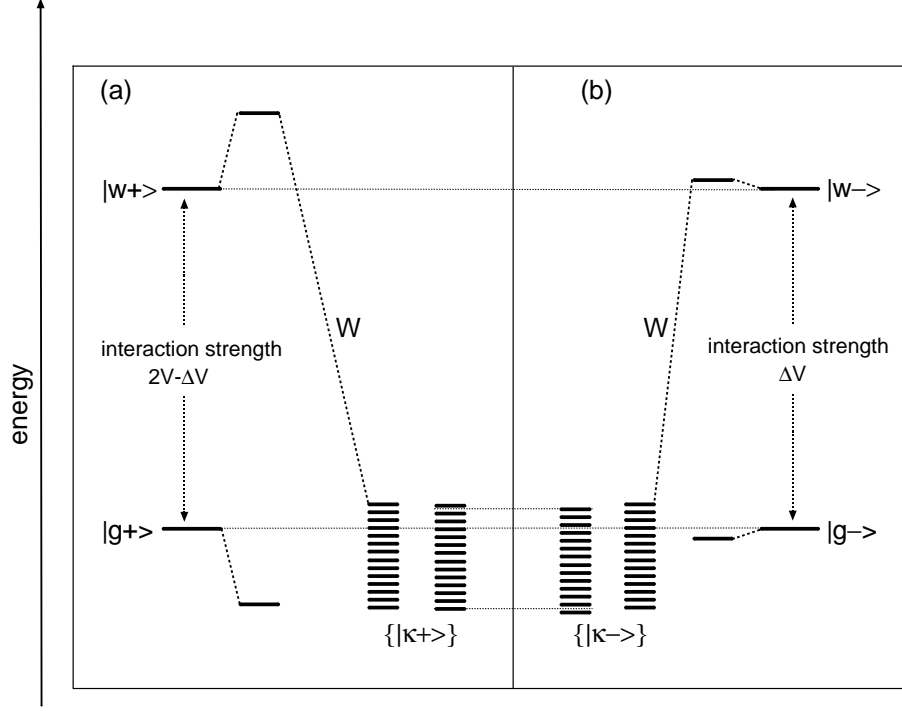


FIG. 3: Schematic energy levels resulting from coupling between the transformed basis states, belonging to the  $\{+\}$  (a) and  $\{-\}$  (b) subsystems (eqs. 9 and 11). The degeneracy between the transformed continua  $\{|\kappa+\rangle\}$  and  $\{|\kappa-\rangle\}$  is lifted due to coupling to  $|w+\rangle$  (a) and to  $|w-\rangle$  (b), respectively. The "particle" in the  $|g-\rangle$ -component alone stays approximately on-shell with the environmental states because of the weaker interaction of the order of  $\Delta V$  with  $|w-\rangle$ .

## B. Coupling regimes

The characteristics of the time development of a wave packet starting in the "particle" state  $|g_\alpha\rangle$  are determined by the Hamiltonian matrix element between the initial state  $|g_\alpha\rangle$  and the eigenstates  $\{|\tilde{\kappa}\pm\rangle\}$  derived from the environmental states. This matrix element might be estimated as follows, if the coupling between the gateway state  $|w_\alpha\rangle$  and the environmental state  $|\kappa_\alpha\rangle$  is weak enough so that perturbation theory can be used to calculate the coefficients  $\langle\tilde{\kappa}\pm|w\pm\rangle$ :

$$\begin{aligned}\langle\tilde{\kappa}-|H|g_\alpha\rangle &\approx \langle\tilde{\kappa}-|H|w-\rangle\langle w-|g_\alpha\rangle + \langle\tilde{\kappa}-|w-\rangle\langle w-|H|g_\alpha\rangle \\ &\approx W \times 0 + \frac{W}{E_w} \frac{1}{\sqrt{2}} \Delta V\end{aligned}\tag{14}$$

$$\langle\tilde{\kappa}+|H|g_\alpha\rangle \approx \langle\tilde{\kappa}+|H|w+\rangle\langle w+|g_\alpha\rangle + \langle\tilde{\kappa}+|w+\rangle\langle w+|H|g_\alpha\rangle$$

$$\approx W \times 0 + \frac{W}{E_w} \frac{1}{\sqrt{2}} (2V - \Delta V) \quad (15)$$

These estimates serve only to define regimes of different coupling strength of  $|g_\alpha\rangle$  to the continuum. In table II ranges of values of the coupling parameters between the initial particle state  $|g_\alpha\rangle$  and the environmental states belonging to the two continua  $\{+\}$  and  $\{-\}$  are indicated. The second column includes intervals for the values of  $\Delta V$ , proportional to the coupling strength to the  $\{|\tilde{\kappa}-\rangle\}$  states. In the third column intervals for  $2V - \Delta V$ , proportional to the coupling strength to  $\{|\tilde{\kappa}+\rangle\}$ , are summarized.

TABLE II: Regimes for different kinds of dynamics of a particle starting in state  $|g_\alpha\rangle$ , in interaction with the continua of environmental states  $\{|\tilde{\kappa}-\rangle\}$  and  $\{|\tilde{\kappa}+\rangle\}$ .

regime	$\langle \tilde{\kappa}-   H   g_\alpha \rangle \frac{\sqrt{2}E_w}{W} = \Delta V$	$\langle \tilde{\kappa}+   H   g_\alpha \rangle \frac{\sqrt{2}E_w}{W} = 2V - \Delta V$
slow Rabi oscillations	$V \dots \frac{5}{6}V$	$V \dots \frac{7}{6}V$
faster Rabi oscillations	$\frac{5}{6}V \dots \frac{1}{2}V$	$\frac{7}{6}V \dots \frac{3}{2}V$
telegraph	$\frac{1}{2}V \dots \frac{1}{6}V$	$\frac{3}{2}V \dots \frac{11}{6}V$
bonding	$\frac{1}{6}V \dots 0$	$\frac{11}{6}V \dots 2V$

Illustrations of these regimes are displayed in the three horizontal panels in fig. 2 for three different choices of the parameter  $V - \Delta V$ . In the regime of slow Rabi oscillations the hopping matrix element in the Hamiltonian  $V - \Delta V$  for switching between the  $\alpha$ - and the  $\beta$ -side is near zero.  $|g_\alpha\rangle$  couples with approximately equal strength  $V$ , which is rather large, to the  $\{|\tilde{\kappa}+\rangle\}$  and  $\{|\tilde{\kappa}-\rangle\}$  continua. The spectral distribution of  $|g_\alpha\rangle$  in the two continua is defined as:

$$\rho_{g_\alpha}(E) = \sum_{\tilde{\kappa}\pm} |\langle \tilde{\kappa}\pm | g_\alpha \rangle|^2 \delta(E - E_{\kappa\pm}) \quad (16)$$

It is rather broad near the energy shell and exhibits approximately equal weights in the two continua (cf. fig. 2, upper right panel). The "particle" oscillates slowly between the two sides (fig. 2, upper central panel). The long oscillation time is determined by the off-shell environmental states, whose degeneracy is only very slightly lifted because the coupling to

both environmental continua  $\{|\tilde{\kappa}-\rangle\}$  and  $\{|\tilde{\kappa}+\rangle\}$  is nearly equally strong. The slow Rabi oscillation is superposed by telegraph-like jumps, the jump time being determined by the value of  $\Delta\varepsilon$  near the energy shell.

In the regime of faster Rabi oscillations,  $V - \Delta V$  deviates significantly from zero. The coupling of  $|g_\alpha\rangle$  to the  $\{|\tilde{\kappa}+\rangle\}$  continuum is already significantly stronger than to the  $\{|\tilde{\kappa}-\rangle\}$  continuum. The spectral weight of  $|g_\alpha\rangle$  in the  $\{|\tilde{\kappa}+\rangle\}$  continuum is therefore shifted from the on-shell region to lower energies and the spectral weight near the energy shell is significantly smaller than in the  $\{|\tilde{\kappa}-\rangle\}$  continuum. No illustration of this regime is given in this paper.

In the region where the telegraph-like switching between sides occurs, the difference between the coupling to the  $\{|\tilde{\kappa}+\rangle\}$  and  $\{|\tilde{\kappa}-\rangle\}$  continua increases. The coupling to the  $\{|\tilde{\kappa}-\rangle\}$  continuum becomes now so small that the spectral distribution of  $|g_\alpha\rangle$  in the  $\{|\tilde{\kappa}-\rangle\}$  continuum is represented by a narrow Lorentzian (fig. 2, middle right panel) responsible for the telegraph signal in the middle central panel, as explained below. The long time transitions are no more discernible because the time development is dominated by the on-shell eigenstates derived from environmental states in the  $\{|\tilde{\kappa}-\rangle\}$  continuum. This yields the telegraph-like behaviour.

In the bonding regime  $V - \Delta V$  equals approximately  $V$  and the coupling between the  $\alpha$  and  $\beta$  sides is so strong that  $|g_\alpha\rangle$  and  $|g_\beta\rangle$  form a linear combination similar to a chemical bond (fig. 2, low right panel). The "particle" is now on the two sides at the same time. There are then no long-time transitions between the  $\alpha$  and the  $\beta$  side, though telegraph-like variations of the occupation of side  $\alpha$  are still discernible. (fig. 2, low central panel).

### C. Diagonalization in the case of a degenerate continuum

We first demonstrate that the telegraph signals are a consequence of the environmental states giving rise to energetically close spaced quasi-continuum states. In the case that all environmental states are degenerate only energetically well separated off-shell eigenstates are coupled to the gateway states giving rise to high frequency sine-like Rabi-oscillations.

We calculate the antisymmetric eigenstates for the degenerate environmental states. Defining the projected state  $|w_{\kappa}-\rangle$

$$|w_{\kappa}-\rangle = \frac{1}{\sqrt{N}} \sum_{\kappa-} |\kappa-\rangle \quad (17)$$

the Hamiltonian in the anti-symmetric subspace takes the form

	$ w-\rangle$	$ w_{\kappa}-\rangle$	$ g-\rangle$
$\langle w- $	$E_w$	$\sqrt{N}W$	$\Delta V$
$\langle w_{\kappa}- $	$\sqrt{N}W$	$0$	$0$
$\langle g- $	$\Delta V$	$0$	$0$

$N$  is the number of degenerate environmental states. This reduces to a  $2 \times 2$ -system by defining

$$|w_{\kappa g}-\rangle = \frac{\sqrt{N}W |w_{\kappa}-\rangle + \Delta V |g-\rangle}{\sqrt{NW^2 + (\Delta V)^2}}. \quad (18)$$

Orthogonalizing  $|g-\rangle$  to  $|w_{\kappa g}-\rangle$

$$|g_{\perp}-\rangle = \sqrt{\frac{NW^2 + (\Delta V)^2}{NW^2}} (|g-\rangle - \langle w_{\kappa g}-|g-\rangle |w_{\kappa g}-\rangle), \quad (19)$$

the Hamiltonian matrix transforms into

	$ w-\rangle$	$ w_{\kappa g}-\rangle$	$ g_{\perp}-\rangle$
$\langle w- $	$E_w$	$\sqrt{NW^2 + (\Delta V)^2}$	$0$
$\langle w_{\kappa g}- $	$\sqrt{NW^2 + (\Delta V)^2}$	$0$	$0$
$\langle g_{\perp}- $	$0$	$0$	$0$

The eigenvalues are:

$$\begin{aligned} E_1 &= 0 \\ E_{2/3} &= \frac{E_w}{2} \pm \frac{E_w}{2} \sqrt{1 + \frac{4(NW^2 + (\Delta V)^2)}{E_w^2}}. \end{aligned} \quad (20)$$

$E_3$  is the energy of the  $|w_{\kappa g}-\rangle$  derived eigenstate and is roughly equal to

$$E_3 \approx -\frac{NW^2 + (\Delta V)^2}{E_w} \quad (21)$$

which, though smaller in magnitude than  $E_w$ , is energetically well separated from the on-shell energy zero.

Orthogonalizing the environmental states to  $|w_{\kappa g}-\rangle$

$$|\kappa_{\perp}-\rangle = \frac{1}{\sqrt{1 - |\langle \kappa- | w_{\kappa g}-\rangle|^2}} \left( |\kappa- \rangle - \frac{W}{\sqrt{NW^2 + (\Delta V)^2}} |w_{\kappa g}-\rangle \right), \quad (22)$$

the antisymmetric states are split in two separated and orthogonal subspaces  $\{|w-\rangle, |w_{\kappa g}-\rangle\}$  and  $\{|g_{\perp}-\rangle, |\kappa_{\perp}-\rangle\}$ , where the latter is energetically on-shell at energy zero and the former is energetically off-shell.  $\langle \kappa- | w_{\kappa g}-\rangle$  is obtained from eq. (18) as

$$\begin{aligned} \langle \kappa- | w_{\kappa g}-\rangle &= \frac{\sqrt{NW} \frac{1}{\sqrt{N}}}{\sqrt{NW^2 + (\Delta V)^2}} \\ &= \frac{W}{\sqrt{NW^2 + (\Delta V)^2}} \end{aligned} \quad (23)$$

which for the results of the center panel in the second row of fig. 2 is roughly  $5 \times 10^{-2}$ .

## D. Interaction in the on-shell subspace

### 1. Hamiltonian matrix elements in the on-shell subspace

We now investigate the interaction of the  $|g_{\perp}-\rangle$ -state with the  $\{|\kappa_{\perp}-\rangle\}$ -states for the *non*-degenerate environmental states continuum using two approximations:

1. The  $\{|g_{\perp}-\rangle, |\kappa_{\perp}-\rangle\}$ -states are mutually orthogonal.
2. The Hamiltonian matrix elements between the  $\{|w-\rangle, |w_{\kappa g}-\rangle\}$  subspace and the  $\{|g_{\perp}-\rangle, |\kappa_{\perp}-\rangle\}$  subspace vanish.

The first assumption is violated to order  $N^{-1}$ , which becomes obvious by calculating the overlap from eqs. (19) and (22):

$$\begin{aligned} \langle \kappa_{\perp}- | g_{\perp}-\rangle &= \sqrt{\frac{NW^2 + (\Delta V)^2}{NW^2}} \sqrt{\frac{NW^2 + (\Delta V)^2}{(N-1)W^2 + (\Delta V)^2}} \\ &\times \left( \langle \kappa- | g- \rangle - \frac{2W \langle w_{\kappa g}- | g- \rangle}{\sqrt{NW^2 + (\Delta V)^2}} - \langle w_{\kappa g}- | g- \rangle \langle \kappa- | w_{\kappa g}- \rangle \right) \end{aligned} \quad (24)$$

where

$$\langle \kappa- | g- \rangle = 0 \quad (25)$$

$$\langle g- | w_{\kappa g}- \rangle = \frac{\Delta V}{\sqrt{NW^2 + (\Delta V)^2}} \quad (26)$$

and  $\langle \kappa - | w_{\kappa g} - \rangle = \frac{W}{\sqrt{NW^2 + (\Delta V)^2}}$  according to eq. (23).

The second assumption is violated to order  $N^{-\frac{1}{2}}\Delta\varepsilon$ . So for increasing number of environmental states and decreasing energetic separation of the environmental states, the approximations become arbitrarily well fulfilled.

We need the Hamiltonian matrix element between  $|g_{\perp}-\rangle$  and  $|\kappa_{\perp}-\rangle$ :

$$\begin{aligned}\langle \kappa_{\perp}- | H | g_{\perp}- \rangle &= \sqrt{\frac{NW^2 + (\Delta V)^2}{NW^2}} \left( \langle \kappa_{\perp}- | H | g- \rangle - \langle w_{\kappa g}- | g- \rangle \langle \kappa_{\perp}- | H | w_{\kappa g}- \rangle \right) \\ &= \sqrt{\frac{NW^2 + (\Delta V)^2}{NW^2}} \left( \frac{1}{\sqrt{1 - |\langle \kappa- | w_{\kappa g}- \rangle|^2}} \langle w_{\kappa g}- | \kappa- \rangle \langle w_{\kappa g}- | H | g- \rangle \right. \\ &\quad \left. - \langle w_{\kappa g}- | g- \rangle \langle \kappa_{\perp}- | H | w_{\kappa g}- \rangle \right)\end{aligned}\quad (27)$$

The Hamiltonian matrix elements appearing in this expression are evaluated as follows:

$$\langle w_{\kappa g}- | H | g- \rangle = \sqrt{\frac{NW^2}{NW^2 + (\Delta V)^2}} \langle w_{\kappa}- | H | w_{\kappa g}- \rangle = 0 \quad (28)$$

$$\begin{aligned}\langle \kappa_{\perp}- | H | w_{\kappa g}- \rangle &= \frac{\sqrt{NW}}{\sqrt{(N-1)W^2 + (\Delta V)^2}} \left( \langle \kappa- | H | w_{\kappa}- \rangle - \langle w_{\kappa g}- | \kappa- \rangle \langle w_{\kappa}- | H | w_{\kappa g}- \rangle \right) \\ &= \frac{WE_{\kappa-}}{\sqrt{(N-1)W^2 + (\Delta V)^2}}\end{aligned}\quad (29)$$

where in the last line we used eq. (17). Inserting in eq. (27) yields:

$$\langle \kappa_{\perp}- | H | g_{\perp}- \rangle = -\frac{\Delta V E_{\kappa-}}{\sqrt{N(N-1)W^2 + N(\Delta V)^2}} \quad (30)$$

which for the results of the center panel in the second row of fig. 2 is roughly  $10^{-2} \times E_{\kappa-}$ .

$$\begin{aligned}\langle \lambda_{\perp}- | H | \kappa_{\perp}- \rangle &= \frac{NW^2 + (\Delta V)^2}{(N-1)W^2 + (\Delta V)^2} \\ &\times \left( \langle \lambda- | H | \kappa- \rangle - \frac{W}{\sqrt{NW^2 + (\Delta V)^2}} \left( \langle \lambda- | H | w_{\kappa g}- \rangle + \langle \kappa- | H | w_{\kappa g}- \rangle \right) \right) \\ &= \frac{NW^2 + (\Delta V)^2}{(N-1)W^2 + (\Delta V)^2} \left( E_{\kappa-} \delta_{\kappa\lambda} - \frac{W^2}{NW^2 + (\Delta V)^2} (E_{\kappa-} + E_{\lambda-}) \right)\end{aligned}\quad (31)$$

which for the results of the center panel in the second row of fig. 2 is roughly  $E_{\kappa-}\delta_{\kappa\lambda} - \frac{1}{N}(E_{\kappa-} + E_{\lambda-})$ . Here we have used:

$$\begin{aligned}
\langle \lambda- | H | w_{\kappa g}- \rangle &= \frac{1}{\sqrt{NW^2 + (\Delta V)^2}} \left( \sqrt{NW} \langle \lambda- | H | w_{\kappa-} \rangle + \Delta V \langle \lambda- | H | g- \rangle \right) \\
&= \frac{1}{\sqrt{NW^2 + (\Delta V)^2}} \left( \frac{\sqrt{NW}}{\sqrt{N}} \langle \lambda- | H | \lambda- \rangle \right) \\
&= \frac{WE_{\lambda-}}{\sqrt{NW^2 + (\Delta V)^2}}
\end{aligned} \tag{32}$$

## 2. Projection of remote state on environmental eigenstates

Environmental eigenstates (exact or approximate) are denoted as  $|\tilde{\kappa}_{\perp}-\rangle$ . We evaluate the coefficient  $\langle g_{\perp}- | \tilde{\kappa}_{\perp}- \rangle$  using the Lippmann-Schwinger equation [15]:

$$\begin{aligned}
\langle g_{\perp}- | \tilde{\kappa}_{\perp}- \rangle &= \langle g_{\perp}- | \kappa_{\perp}- \rangle \\
&+ \sum_{\lambda} \langle g_{\perp}- | G(E = E_{\tilde{\kappa}-}) | \lambda_{\perp}- \rangle \langle \lambda_{\perp}- | H_{\perp} - H_o | \kappa_{\perp}- \rangle
\end{aligned} \tag{33}$$

where  $H_o$  is the last but one line of eq. (13) and the summation over  $\lambda$  is over all states in the anti-symmetric on-shell continuum.  $G(E) = (E - H_{\perp})^{-1}$  is the Green operator. Using Dyson's equation one obtains

$$\begin{aligned}
\langle g_{\perp}- | \tilde{\kappa}_{\perp}- \rangle &= \langle g_{\perp}- | \kappa_{\perp}- \rangle + \langle g_{\perp}- | G_o(E = E_{\tilde{\kappa}-}) | g_{\perp}- \rangle \langle g_{\perp}- | H_{\perp} - H_o | \kappa_{\perp}- \rangle \\
&+ \sum_{\lambda, \mu} \langle g_{\perp}- | G_o(E = E_{\tilde{\kappa}-}) | g_{\perp}- \rangle \langle g_{\perp}- | H_{\perp} - H_o | \lambda_{\perp}- \rangle \\
&\times \langle \lambda_{\perp}- | G(E = E_{\tilde{\kappa}-}) | \mu_{\perp}- \rangle \langle \mu_{\perp}- | H_{\perp} - H_o | \kappa_{\perp}- \rangle
\end{aligned} \tag{34}$$

where  $G_o(E) = (E - H_o)^{-1}$ . Eq. (33) describes the scattering of a "particle" incoming in  $|\kappa_{\perp}-\rangle$  from the perturbation provided by the remote state  $|g_{\perp}-\rangle$  and the environmental states  $|\lambda_{\perp}-\rangle$ . Obviously outgoing boundary conditions are applied, although this is not indicated explicitly on the Green function. The Green function has to be evaluated at the energy of the environmental state under consideration.

The first term on the r.h.s. of eq. (34) vanishes, because the  $\perp$ -states are assumed to be orthogonal. In the second term on the r.h.s. of eq. (34) the  $E_{\kappa-}$ -dependence is cancelled and for the results of the center panel in the second row of fig. 2 the line width resulting from



this term would be of order  $10^{-4} \times \Delta\varepsilon \approx 10^{-10}$  which is at least four orders of magnitude too small compared to the values obtained numerically.

In order to estimate the third term on the r.h.s. of eq. (34) we could replace the exact Green operator  $G$  by  $G_o$  so that the third term becomes:

$$\begin{aligned} \langle g_{\perp-} | \tilde{\kappa}_{\perp-} \rangle &\approx \frac{1}{E_{\kappa-}} \frac{\Delta V}{\sqrt{(N-1)W^2 + (\Delta V)^2}} \sum_{\lambda} E_{\lambda-} \frac{1}{NE_{\lambda-}} (E_{\kappa-} + E_{\lambda-}) \\ &\approx \frac{1}{NE_{\kappa-}} \frac{\Delta V}{\sqrt{(N-1)W^2 + (\Delta V)^2}} \left( \sum_{\lambda} E_{\lambda-} + NE_{\kappa-} \right) \\ &\approx \frac{\Delta V}{\sqrt{(N-1)W^2 + (\Delta V)^2}} \end{aligned}$$

which is independent of  $E_{\kappa-}$  and for the results of the center panel in the second row of fig. 2 roughly of order  $5 \times 10^{-2}$ . The line width resulting from this term would be of order  $10^{-2} \times \Delta\varepsilon \approx 10^{-8}$  and too small.

Hence replacing  $G$  by  $G_o$  in eq. (34) does not yield any improvement. This estimate shows that the telegraph signals can only appear in higher order and therefore we substitute Dyson's equation for the exact Green operator  $G$  in the third term on the r.h.s. of eq. (34):

$$\begin{aligned} \langle \lambda_{\perp-} | G | \mu_{\perp-} \rangle &= \langle \lambda_{\perp-} | G_o | \mu_{\perp-} \rangle \\ &+ \langle \lambda_{\perp-} | G_o | \lambda_{\perp-} \rangle \sum_{\nu} \langle \lambda_{\perp-} | H_- - H_o | \nu_{\perp-} \rangle \langle \nu_{\perp-} | G | \mu_{\perp-} \rangle \end{aligned} \quad (35)$$

The first term reproduces the previous estimate. Re-inserting repeatedly this expression on the r.h.s. of eq. (35) one obtains the infinite series

$$\begin{aligned} \langle \lambda_{\perp-} | G | \mu_{\perp-} \rangle &= \langle \lambda_{\perp-} | G_o | \lambda_{\perp-} \rangle \langle \lambda_{\perp-} | H_- - H_o | \mu_{\perp-} \rangle \langle \mu_{\perp-} | G_o | \mu_{\perp-} \rangle \\ &+ \langle \lambda_{\perp-} | G_o | \lambda_{\perp-} \rangle \sum_{\nu} \langle \lambda_{\perp-} | H_- - H_o | \nu_{\perp-} \rangle \langle \nu_{\perp-} | G_o | \nu_{\perp-} \rangle \\ &\times \langle \nu_{\perp-} | H_- - H_o | \mu_{\perp-} \rangle \langle \mu_{\perp-} | G_o | \mu_{\perp-} \rangle \\ &+ \langle \lambda_{\perp-} | G_o | \lambda_{\perp-} \rangle \sum_{\nu} \langle \lambda_{\perp-} | H_- - H_o | \nu_{\perp-} \rangle \langle \nu_{\perp-} | G_o | \nu_{\perp-} \rangle \\ &\times \sum_{\iota} \langle \nu_{\perp-} | H_- - H_o | \iota_{\perp-} \rangle \langle \iota_{\perp-} | G_o | \iota_{\perp-} \rangle \\ &\times \langle \iota_{\perp-} | H_- - H_o | \mu_{\perp-} \rangle \langle \mu_{\perp-} | G_o | \mu_{\perp-} \rangle \\ &+ \dots \end{aligned} \quad (36)$$

Assuming short range scattering

$$\langle \iota_{\perp-} | H_- - H_o | \mu_{\perp-} \rangle = U \quad (37)$$

the series can be written in the form

$$\langle \lambda_{\perp-} | G | \mu_{\perp-} \rangle = \langle \lambda_{\perp-} | G_o | \lambda_{\perp-} \rangle \langle \mu_{\perp-} | G_o | \mu_{\perp-} \rangle \sum_{k=1}^{\infty} U^k \left( \sum_{\iota} \langle \iota_{\perp-} | G_o | \iota_{\perp-} \rangle \right)^{k-1} \quad (38)$$

The infinite series can be formally summed to yield:

$$\langle \lambda_{\perp-} | G | \mu_{\perp-} \rangle = \langle \lambda_{\perp-} | G_o | \lambda_{\perp-} \rangle \langle \mu_{\perp-} | G_o | \mu_{\perp-} \rangle \frac{U}{1 - U \sum_{\iota} \langle \iota_{\perp-} | G_o | \iota_{\perp-} \rangle} \quad (39)$$

$\sum_{\iota} \langle \iota_{\perp-} | G_o | \iota_{\perp-} \rangle$  is directly connected to the density of on-shell environmental states:

$$\sum_{\iota} \langle \iota_{\perp-} | G_o | \iota_{\perp-} \rangle = \mathcal{P} \sum_{\iota} \frac{1}{E - E_{\iota-}} - i\pi \sum_{\iota} \delta(E - E_{\iota-}) \quad (40)$$

$$= \mathcal{H}(\Gamma(E)) - i\Gamma(E) \quad (41)$$

$\mathcal{P}$  and  $\mathcal{H}$  indicate the principal part and the Hilbert transform, respectively.  $\Gamma(E)$  is defined by:

$$\begin{aligned} \Gamma(E) &= \frac{\pi}{\Delta\epsilon} \text{ for } |E| < a \\ &= 0 \quad \text{elsewhere} \end{aligned} \quad (42)$$

$2a$  is the bandwidth of the environmental states.

The principal value can be estimated by evaluating the integral

$$\int_{-a}^a \frac{dE_{\iota-}}{E - E_{\iota-}} = \ln \left| \frac{E + a}{E - a} \right| \quad (43)$$

which is zero on-shell and negligible for the environmental states near the energy shell. For the results of the center panel in the second row of fig. 2 the principle part is negligible and  $U \sum_{\iota} \langle \iota_{\perp-} | G_o | \iota_{\perp-} \rangle$  is smaller than unity but of the order of unity:

$$U \sum_{\iota} \langle \iota_{\perp-} | G_o | \iota_{\perp-} \rangle = \frac{1}{F} \quad (44)$$

where  $F$  is a positive number greater unity. Writing

$$\begin{aligned} \frac{U}{1 - \frac{1}{F}} &= \frac{FU}{F - 1} \\ &= \frac{1}{(F - 1) \sum_{\iota} \langle \iota_{\perp-} | G_o | \iota_{\perp-} \rangle} \\ &\approx \frac{1}{\sum_{\iota} \langle \iota_{\perp-} | G_o | \iota_{\perp-} \rangle} \end{aligned} \quad (45)$$

the Green function reads:

$$\langle \lambda_{\perp} - | G | \mu_{\perp} - \rangle = i \frac{\Delta \varepsilon}{\pi} \langle \lambda_{\perp} - | G_o | \lambda_{\perp} - \rangle \langle \mu_{\perp} - | G_o | \mu_{\perp} - \rangle \quad (46)$$

Inserting this and eq. (30) in the third term of eq. (34), yields for this term:

$$\begin{aligned} \langle g_{\perp} - | \tilde{\kappa}_{\perp} - \rangle &\approx i \frac{\Delta \varepsilon}{\pi} \frac{\Delta V}{NW} \frac{1}{E_{\kappa-}} \sum_{\lambda, \mu} E_{\lambda-} \frac{1}{E_{\lambda-}} \frac{1}{E_{\mu-}} \frac{E_{\mu-} + E_{\kappa-}}{N} \\ &= i \frac{\Delta \varepsilon}{\pi} \frac{\Delta V}{NW} \frac{1}{E_{\kappa-}} \sum_{\lambda, \mu} \frac{1}{N} \\ &= i \frac{\Delta \varepsilon}{\pi} \frac{\Delta V}{W} \frac{1}{E_{\kappa-}} \end{aligned} \quad (47)$$

This is of order unity and has the right  $E_{\kappa-}$ -dependence to yield the telegraph signals. It is in accordance with the results of the numerical calculations.

According to equation (5) the time dependent wave packet evolving out of  $|g_{\alpha}\rangle$  is then written as

$$|g_{\alpha}(t)\rangle = \langle \tilde{\kappa}_{\perp} - | g_{\perp} - \rangle \langle g_{\perp} - | g - \rangle \langle g - | g_{\alpha} \rangle e^{-iE_{\tilde{\kappa}-}t/\hbar} | \tilde{\kappa}_{\perp} - \rangle \quad (48)$$

Using eqs. (18) and (19) we obtain

$$\begin{aligned} \langle g - | g_{\perp} - \rangle &= \sqrt{\frac{NW^2 + (\Delta V)^2}{NW^2}} \left( 1 - \frac{(\Delta V)^2}{NW^2 + (\Delta V)^2} \right) \\ &= \sqrt{\frac{NW^2}{NW^2 + (\Delta V)^2}} \end{aligned} \quad (49)$$

which is of order unity.

Defining the on-shell projected state

$$|A\kappa-\rangle = \frac{1}{\sqrt{N}} \sum_{\kappa-} | \tilde{\kappa}_{\perp} - \rangle \quad (50)$$

and projecting eq. (48) on  $|A\kappa-\rangle$  one obtains:

$$\begin{aligned} \langle A\kappa- | g_{\alpha}(t) \rangle &= i \frac{\Delta \varepsilon}{\pi} \frac{\Delta V}{W} \sum_{\tilde{\kappa}-} \frac{1}{E_{\kappa-}} \sqrt{\frac{NW^2}{NW^2 + (\Delta V)^2}} \frac{1}{\sqrt{2}} \frac{1}{\sqrt{N}} e^{-iE_{\tilde{\kappa}-}t/\hbar} \\ &= \frac{1}{\pi} \frac{\Delta V}{W} \frac{1}{\sqrt{2N}} \sqrt{\frac{NW^2}{NW^2 + (\Delta V)^2}} \\ &\times \left( \sin(\Delta \varepsilon t/\hbar) + \frac{\sin(3\Delta \varepsilon t/\hbar)}{3} + \frac{\sin(5\Delta \varepsilon t/\hbar)}{5} + \dots \right) \end{aligned} \quad (51)$$

yielding the telegraph signal. A step-like periodic function  $f(x)$ , resembling a telegraph signal with a constant period, has the following Fourier expansion;

$$f(x) = \sin x + \frac{\sin 3x}{3} + \frac{\sin 5x}{5} + \dots \quad (52)$$

Hence the superposition of sine-functions with frequencies, which are multiples of a ground frequency, yields a telegraph-like behaviour.

Supporting evidence comes from the spectral distribution of the entanglement of the initial "particle" state  $|g_\alpha\rangle$  in the band of environmental states

$$\rho_{g\alpha}(E) = \sum_{\tilde{\kappa}\pm} |\langle \tilde{\kappa}\pm | g_\alpha \rangle|^2 \delta(E - E_{\kappa\pm}) \quad (53)$$

$$= -\frac{1}{\pi} \text{Im} G_{g\alpha}(E) \quad (54)$$

where the Green function  $G_{g\alpha}(E)$  is defined by:

$$G_{g\alpha}(E) = \frac{1}{E - E_{g\alpha} - \Sigma_{g\alpha}} \quad (55)$$

For energies close to the energy shell the self-energy  $\Sigma_{g\alpha}$  is given by:

$$\Sigma_{g\alpha} = \mathcal{P} \sum_{\kappa\pm} \frac{|\langle \tilde{\kappa}_\perp \pm | H | g_\alpha \rangle|^2}{E - E_{\kappa\pm}} - i\pi \sum_{\kappa\pm} |\langle \tilde{\kappa}_\perp \pm | H | g_\alpha \rangle|^2 \delta(E - E_{\kappa\pm}) \quad (56)$$

$\mathcal{P}$  denotes the principal part. The imaginary part of the Green function is:

$$\text{Im} G_{g\alpha}(E) = \frac{\text{Im} \Sigma_{g\alpha}}{(E - E_{g\alpha} - \text{Re} \Sigma_{g\alpha})^2 + (\text{Im} \Sigma_{g\alpha})^2} \quad (57)$$

The spectral distributions are plotted in fig. 2 in the panels on the right hand side for the three parameter choices. As it was demonstrated in a previous paragraph, in the telegraph regime (plot in the middle central panel of fig. 2) just the anti-symmetric "particle" states remain significantly on-shell. This explains why the spectral weight of the initial state on the on-shell eigenstates, derived from the components  $\{|\kappa-\rangle\}$ , is non-zero and larger than its spectral weight on eigenstates, derived from environmental states components  $\{|\kappa+\rangle\}$ . This is obvious from the alternating small and large values of the spectral weight of  $|g_\alpha\rangle$  on eigenstates. Therefore, the initial "particle" state acquires, in its time development, environmental states components with multiple energy differences, hence its time development must resemble a telegraph signal.

The resonances in the spectral distributions are of Lorentzian shape. The time development of the amplitude of the wave packet as given in eq. (48) is directly connected with a sharp resonance of Lorentzian shape. Such sharp resonances only arise, if the "particle" state interacts very weakly and locally in space with a continuum degenerate in energy. The locality of the interaction guarantees that the coupling does not vary over the continuum. Only then a Lorentzian shape is obtained. The weak interaction guarantees that the resonance is centered on the energy shell.

The telegraph signal in our example is a sudden change of state of the whole system. After a time interval suddenly the "particle" attempts to change side. Sometimes the attempt is successful, but not every attempt leads to a side change as it can be seen in the plot in fig. 2 (middle central panel) at times around 4000 seconds .

### E. Possible application

Possible application of our theory is in the field of surface phenomena, where telegraph signals have indeed been observed, associated with state changes in bistable systems. At low temperature when the diffusion of adsorbates on solid surfaces is slowed down, the movement of single atoms and molecules can be traced with scanning tunnelling microscopy (STM). In these experiments much faster telegraph-signal-like jumps of the adsorbate from its adsorption site to a neighbouring one are observed, compared to the time the adsorbate is localized on each adsorption site (cf. for instance the hopping time of a hydrogen atom on Cu(100) [16] and of one CO molecule in a chevron structure on Cu(111) [6]). In a current-induced hydrogen tautomerization reaction of naphthalocyanine adsorbed on a NaCl/Cu(111) surface two hydrogen atoms in the inner cavity change place reversibly in a telegraph manner at temperature 5K [5]. A telegraph signal is observed by Repp et al. [17] as an adsorbed Au atom on a NaCl/Cu(111) surface switches between a higher and a lower oxidation states. Current-induced transitions to coverage-dependent excited states of H<sub>2</sub> on Cu(111) at 5K [18], as well as reversible rotational excitation of O<sub>2</sub> on Pt(111) [19], C<sub>2</sub>HD on Cu(100) [20] and dibutyl sulfide on Cu(111) and Au(111) [7, 8], transition between distinct current states due to conformational changes [9, 21–23], are examples of telegraph-signal-like behaviour

of adsorbates in the low temperature STM. The time oscillations of the Hall photovoltage across different pairs of contacts in a Hall bar geometry show a statistical telegraph signal [4].

## V. CONCLUSION

The quantum theory of the dynamics of a "particle" coupling to a continuum of environmental states, suggested in the present communication, yields a telegraph-signal-like time development of a bistable system as a solution of the time dependent Schrödinger equation. The coherent time development of the two-state system entangled to environmental states of different physical nature reproduces the telegraph behaviour, observed in experiments of very different kind. The telegraph signal originates in our theory due to a weak and local interaction of discrete degrees of freedom with on-shell environmental states of high density of states. The time scale of the telegraph signal is determined by the energy separation of two adjacent environmental states and can vary over a large range from picoseconds to seconds.

- 
- [1] E. Simoen and C. Claeys, *Mat. Sci. Engineering B* **91-92**, 136 (2002).
  - [2] M. Nirmal, B. O. Dabbousi, M. G. Bawendi, J. J. Macklin, J. K. Trautman, T. D. Harris, and L. E. Brus, *Nature* **383**, 802 (1996).
  - [3] S. Reick, K. Mølmer, W. Alt, M. Eckstein, T. Kampschulte, L. Kong, R. Reimann, A. Thobe, A. Widera, and D. Meschede, *J. Opt. Soc. Am. B* **27**, A152 (2010).
  - [4] S. I. Dorozhkin, L. Pfeiffer, K. West, K. von Klitzing, and J. H. Smet, *Nature Physics* **7**, 336 (2011).
  - [5] P. Liljeroth, J. Repp, and G. Meyer, *Science* **317**, 1203 (2007).
  - [6] A. J. Heinrich, C. P. Lutz, J. A. Gupta, and D. M. Eigler, *Science* **298**, 1381 (2002).
  - [7] A. D. Jewell, H. L. Tierney, A. E. Baber, E. V. Iski, M. M. Laha, and E. C. H. Sykes, *J. Phys. Cond. Matter* **22**, 264006 (2010).
  - [8] H. L. Tierney, A. E. Baber, A. D. Jewell, E. V. Iski, M. B. Boucher, and E. C. H. Sykes, *Chem. - Eur. J.* **15**, 9678 (2009).

- [9] Ch. Nacci, S. Folsch, K. Zenichowski, J. Dokic, T. Klamroth, and P. Saalfrank, *Nano Lett.* **9**, 2996 (2009).
- [10] A. Suarez and R. Silbey, *J. Phys. Chem.* **98**, 7329 (1994).
- [11] G. Auletta, *Foundations and Interpretation of Quantum Mechanics: In the Light of a Critical-Historical Analysis of the Problems and of a Synthesis of the Results* (World Sci. Publ. Co, Singapore, 2001).
- [12] A. Böhm, *Quantum Mechanics* (Springer, Berlin, 1979).
- [13] D. Drakova and G. Doyen, *e-J. Surf. Sci. Nanotech.* **8**, 6 (2010).
- [14] G. Doyen and D. Drakova, *J. Phys.: Conf. Series* **306**, 012033 (2011); D. Drakova and G. Doyen, *J. Phys.: Conf. Series* **306**, 012068 (2011).
- [15] B. A. Lippmann and J. Schwinger, *Phys. Rev.* **79**, 469 (1950).
- [16] L. J. Lauhon and W. Ho, *Phys. Rev. Lett.* **85**, 4566 (2000); Erratum: L. J. Lauhon and W. Ho, *Phys. Rev. Lett.* **85**, 079901 (2002).
- [17] J. Repp, G. Meyer, F. E. Olsson, and M. Persson, *Science* **305**, 493 (2004).
- [18] J. A. Gupta, C. P. Lutz, A. J. Heinrich, and D. M. Eigler, *Phys. Rev. B* **71**, 115416 (2005).
- [19] B. C. Stipe, M. A. Rezaei, and W. Ho, *Science* **279**, 1907 (1998).
- [20] B. C. Stipe, M. A. Rezaei, and W. Ho, *Phys. Rev. Letters* **82**, 1724 (1999).
- [21] J. Gaudioso, L. J. Lauhon, and W. Ho, *Phys. Rev. Letters* **85**, 1918 (2000).
- [22] J. Gaudioso and W. Ho, *Angew. Chem. Int. Ed.* **40**, 4080 (2001); W. Ho, *J. Chem. Phys.* **117**, 11033 (2002).
- [23] Z. J. Donhauser, B. A. Mantooth, K. F. Kelly, L. A. Bumm, J. D. Monnell, J. J. Stapleton, D. W. Price Jr., A. M. Rawlett, D. L. Allara, J. M. Tour, and P. S. Weiss, *Science* **292**, 2303 (2001).